MECHATRONICS

IJIM

INTERNATIONAL JOURNAL OF

INTELLIGENT MECHATRONICS

DESIGN AND PRODUCTION

VOL. 1 NO. 3

MAY 1995

International Journal of Intelligent Mechatronics: Design and Production,
1(3) May 1995 , pp. 111 – 143, Received February 1995.

DEVELOPMENT OF INTELLIGENT MOBILE ROBOTS FOR SERVICE USE AND MOBILE AUTOMATION SYSTEMS INCLUDING WALL CLIMBING ROBOTS: Pt. 1. FUNDAMENTAL DESIGN PRINCIPLES AND MOTION MODELS.

S.V.ULYANOV,
K. YAMAFUJI
The University of
Electro-
Communications
JAPAN
V.G.GRADETSKY
The Institute for
Problems in Mechanics,
Russian Academy of
Sciences,
RUSSIA
T. FUKUDA
Nagoya Universtiy
JAPAN

Abstract

This paper describes the development of intelligent mobile robot systems for service use including wall climbing robots (WCR). Such robots and robotics complexes are needed because of increasing demands on industrial operations, accident and emergency conditions, and in hazardous or extreme environments. Emergency conditions or hazardous environments may be elevated levels by radioactivity, high temperatures, high gaseous concentrations, etc. The different models of mechanical motion along vertical surfaces by various means, modelling of motion, investigation of maneuverability as well as locomotion, and analysis of mechanical systems for effective execution of different industrial operations are discussed. Methods of facilitating robot motion along vertical surfaces, and advantages and drawbacks of each method are examined. Wall surface mobile robot having multiple suckers on variable structural crawler is developed and tested. Analytical methods for designing maximum stable payload which a walking WCR can carry are examined. Analytical forms of equilibrium conditions, load carrying ability and analysis of stable grasping strategy for walking WCR are investigated. The calculation schemes can be performed on a computer and used to verify the reliability of stable contact between WCR and the surface over the entire path that the WCR traverses. In order to improve manoeuverability and extend functional capabilities, the advanced mobile robotic complex has been developed; an automatically controlled horizontally-mobile robot which is connected to WCR, and a manipulator for providing adhesion of the WCR to the surface and conducting jobs. The complex can be controlled from a single control panel in an autonomous, supervisory, or automatic mode.

Key words: Mobile robot for sevice use, Wall climbing robot, Intelligent control system, Variable structural crawler, Payload capacity

1. INTRODUCTION

At present two classes of mobile robots for service use are distinguished (Asami 1994): (1) Class A (Robots to replace human beings at work in dirty, hazardous and/or tedious operations); and (2) Class B (Robots to operate on/or with human beings to alleviate incommodity or to increase comfort/pleasure). Class A includes operations in hazardous or extreme environment (e.g., radioactive environment, high temperature, underwater, vacum), fire-fighting, military applications, etc. Class B includes office work, medicine, housework, entertainment and others. Developed mobile robots for service use for solving the tasks of class B are shown in Fig.1a and b (Yamafuji et al. 1992). Walking and other types of mobile robots have been the subjects of intensive research. All of these robots have been designed to move over surfaces that make only a small angle with the horizontal. In a number of cases, however, need arises for a robot to move over surface that make fairly large angles-right up to the vertical, negative angles, or even upside down over horizontal surface (the ceiling of a room). This is necessary when fighting fires, painting and repairing the hulls and holds of ships, inspecting large gas and liquid storage tanks or pipe-lines, etc.

Extensive research has been conducted in recent years in developed countries for the purpose of fabricating mobile robots for service use of Class A which are capable of moving along horizontal, inclined or vertical surfaces. Such robots must be capable of overcoming of avoiding obstacles encountered in their paths, or returning to the required initial (start) position, set up to execute the required industrial operations and to perform such execution. Such robots and robotic complexes are needed because of increasing demands on industrial operations, accident and emergency conditions, and conditions that are hazardous or difficult for human operator. Emergency conditions or hazardous environments may have elevated levels of radioactivity, hihg temperature, high gaseous concentrations, etc. It may, for example, be necessary to decontaminate facilities, including walls and floors, to eliminate emergency operations in nuclear-power plants, to fight fires, works in construction, assembly, or paint structures at high elevations or construct a variety of structures, repair ship hulls in dock, etc.

In many cases horizontally-mobile robots or WCR are used separately. However, there are often problems to be treated such as in the case of facility decontamination, when the mobile nechanisms must have a higher degree of mobility and be capable of carying out the required operations by moving along horizontal and vertical surfaces as well as floors.

Research and development of robots with high-mobility, including WCR have been progressing rapidly over the last decade in the supports of national and international programs in Russia, Japan, United States, Great Britain, France, and other nations. Universal vacuum devices (independent of the surface material) are widely used as grippers for gripping vertical surfaces and floors; the robots also use controlled magnetic grippers designed for robot gripping of ferromagnetic surfaces. As example, the most promising way to have robots that move over steep and vertical surfaces is walking robots equipped with special grip-

pers (feet) that ensure the robot to be held on the surface. These grippers may be in this case magnetic feet or vacuum cups. Magnetic feet can only be used when the robot is to be used on ferromagnetic surfaces. Permanent magnets or electromagnets may be used for this purpose. The attractive force produced by the magnets is highly dependent upon the cleanliness of both the surface over which the robot moves and upon the gripper surface, which means that the magnet surface must periodically be cleaned. Whatever permanent magnet grippers are used to hold the robot on the surface, special means are needed to break the foot loose from the surface. Vacuum grippers are more universal and suitable for any fairly smooth surface (metal, concrete, painted surfaces, ceramic tile, etc.). This situation is examined in detail in part 2.

Different companies have had significant results with industrial applications of WCR, including Robotics Ltd., (Russia), Nikki Ltd. Tokyo Gas Ltd., Hitachi, Ishikawa-Harima Heavy Industries (IHI) Ltd. (Japan), International Robotics Technology (USA), Portsmouth Polytechnic (Great Britain), etc.

Mobile robots for service use are distinguished from industrial robots by the following faculties: (1) mobility; (2) maneuverability; (3) intelligence levels; (4) operating ease; (5) adaptability and (6) versatility.

Created by the popular trend toward higher education levels, shortages in the aging specialized labor market, created by the increasing ages of highly skilled technical personnel, and trends toward replacing manual works by robotized operation in hazardous work are factors favoring the market demand for robots for service use.

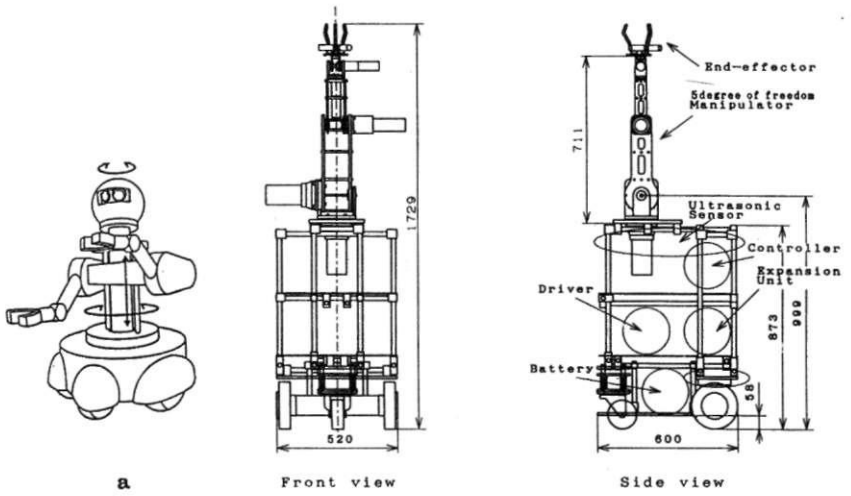

Figure 1. Mobile robots for service use.

Negative factors affecting the robots for service use market include insufficiently rapid development of requisite sensors and of their intelligent faculty, and high cost (Asami 1994).

Further development in this new field of robot engineering permits, to compensate for negative factors has required research aimed at improving mobility and maneuverability of robots, as well as intelligence (sensing, learning, inferring and judging function) and expanding technological capabilities and effective fields of application.

Improvement of mobility and maneuverability allowing robots to advance from floor to wall and from wall to ceiling etc. during movement is of importance for robots in unmanned environments. Certain achievements accomplished on this problem to date however require their own further development. One of the methods improving mobility involses installing a WCR on a mobile carrier-robot (dolly or carriage) capable of moving along horizontal surfaces. The WCR attaches itself to the vertical surfaces automatically in response to correponding control command. The Institute for Problems in Mechanics of the Russian Academy of Sciences, University of Electro-Communications (Japan) and Nagoya University (Japan) have developed different models of a high mobility and reliability robotic complexes with WCR and crawlers. The results of this design development will be discussed in this paper.

The intelligence of the system is improved by installing corresponding sensors (radar, ultrasound, laser, tactile, vision camera, etc.), by establishing feedback, developing special scene analysis algorithms, developing data bases on external environments and autonomous decision making on the basis of fuzzy logic, genetic algorithms and neural networks. This approach to AI control system design for WCR is examined in Part 3. The significant advantages provided by the future development of such systems include the possibility of using them in working environments and in emergencies which are hazardous or difficult for human workers (high radiation, high temperature, toxic or poisonous gases, high elevations for industrial operations as well as other emergency situations).

This paper has four parts and presents results from research devoted to the problem of fabricating WCR: especially, the realization of mechanical motion along vertical surfaces by various means, modelling of intelligent control motion, investigation of maneuverability and locomotion, analysis of mechanical systems for effective execution of different industrial operations including motion from one surface to another at right angle, investigation and development of vauum grippers and mechatronics drive.

In order to improve manoeuvarability and extend functional capabilities, the mobile robotic system is composed of an automatically controlled horizontally-mobile robot, a connected WCR, and a manipulator for providing adhesion of the WCR to the surface (Fig.2). The system can be controlled from a single control panel in an autonomous, supervisory, or automatic mode. The control panel is located in a separate facility at a safe distance from the operations site of the robot in a certain emergency environment (Fig.2 and 3).

As demonstrated by the First In-

ternational Olympiad (Anon 1990) held in September 1990 in Glasgow (Scotland), the achievements in this field are resulted in 2 medals awarded to the Institute for Problems in Mechanics of the Russian Academy of Sciences in this Olympiad.

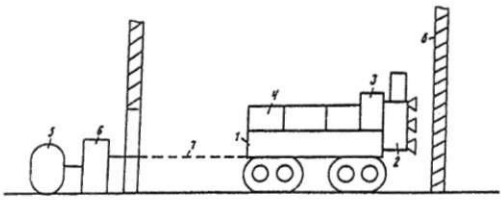

Figure 2. The structure of robotic mobile systems with WCR High mobility robotic system; (1) horizontally-mobile robot; (2) WCR containing industrial equipment; (3) interface between WCR and horizontally-mobile robot; (4) power source; (5) operator; (6) control panel; (7) control channel; (8) working surface.

2. METHODS OF REALIZING WCR MOBILITY ALONG VERTICAL SURFACES AND TYPES OF WCR

The following methods are used to realize the mechanical motion of the transport module along a vertical surface (Gradetsky 1993).

A. The first is a *discrete step method.* In this method, the robot platform travels in discrete steps, with one group of grippers clamping at intervals between the steps and the other group releasing at intervals. Variants of this methods include a discrete step method with uncontrolled locomation speed, and a discrete step method with controlled locomotion speed within each individual step. The advantages of this method is of ease of realization and its performance reliability. The drawbacks are low speed

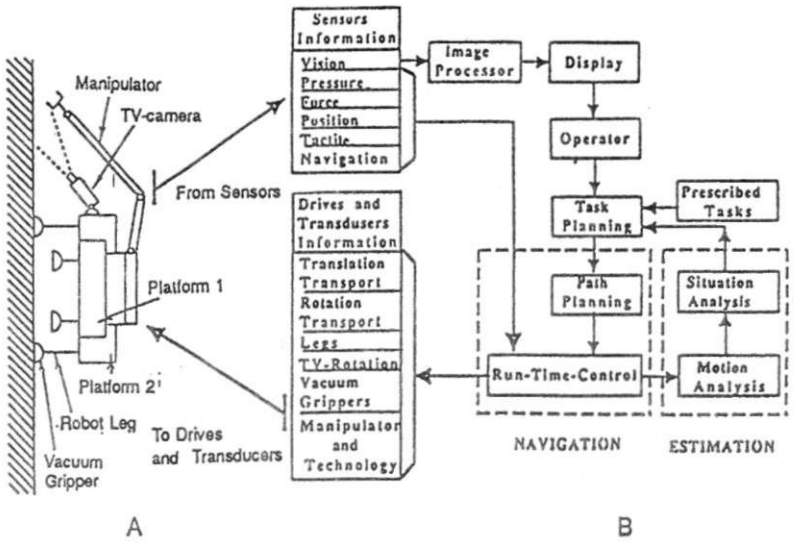

Figure 3. Basic conception of the control system.

and limited functional capabilities. A continuous speed of the robot platform cannot be achieved using this method.

B. The second method of locomotion along vertical surface is *continuous step method.* This method makes possible continuous locomotion of the robot platform in a step mode, whereby one group of grippers initiates gripping and the other group is released without interrupting the platform motion. This method extends the functional capabilities of the robot by achieving a continuous speed of the robot platform, and hence the industrial equipment mounted on the platform. However, the algorithm and the control systems are more complicated.

C. The third method is *the crawler method.* This method makes it possible to obtain a continuous robot platform speed by employing a crawler mechanism. The varieties of this method include a method using internal grippers in the crawler mechanism and the crawler method utilizing indenpendent grippers. In the latter case, the crawler mechanism is used only to initiate robot translational motion within the free range of the drive when the grippers are fixed. The primary advantage of the gripper method of locomotion is its high degree of locomotive mobility and reliability. The drawbacks are increasing complexity and weight.

D. The fourth method of moving along vertical surfaces is *the anthropomorphic method.* In this method, motion is initiated by means of multilink-support members that simulate the motion of living organisms, especially insects. This method requires a large number of degrees of freedom and an advanced control system. The complexity of structural realization in this case reduces the performance reliability of the complex as a whole. However, this method provides the best flexibility for overcoming a variety of obstacles.

E. The fifth method is a particular case of the fourth method and is the *locomotion method over a wall surface by propelling power and thrust force type model.* Two types of propellers are there: those with large diameter thruster as a helicopter rotor, and a small as light plane. However, wind load is larger for the former, and it is dangerous to use it in a strong wind. Therefore, the former is effective to use in a calm or small wind condition.

F. The sixth method of moving along vertical surface is *the parellerogram method.* This method is named after the features of its realization which utilizes the property of a parallelogram which allows alternate motion of its parallel, hinged sides. In this case, there is no need to use two platforms which, in combination with the absence of gripper elevation and descent drives, make this design simple and light. When gripper on one side of the parallelogram is used for clamping, the second side moves in a given direction moving the attached free grippers by sliding along the surface. This method is the fastest, although it has a comparatively low reliability and limited capabilities with respect to industrial applications, since there is no working support platform. Moreover, this design is insufficiently rigid and has limited lift capacity.

As a result, three types of mobile methods for robots have been developed for moving on wall surfaces: (1) the reverse-hovercraft type; (2) walking (wheeled-and legged-type) types; and (3) crawler types.

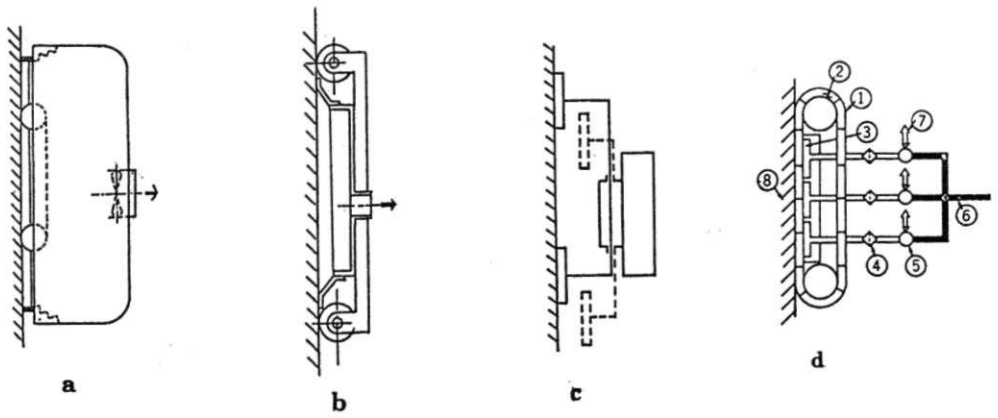

Figure 4. Motion models of WCR's.

In Fig. 4 possible structures of these three types WCR are illustrated. The different types of these structures are examined in Part IV. As shown in (Oomichi 1992, Fukuda 1992a) few of these three types of robots have been put into actual use.

At design of running mechanism for wall surface mobile robot, the following two points became clear (Fukuda 1992): (1) how to prevent fall of the WCR due to gravity; and (2) how to move smoothly. From the analysis of possible motion methods we got the following conclusions for design of locomotive mechanisms. Firsts of all, a way of using magnetic force (Naito 1992, Hirose et al. 1992, Aoyama et al. 1992) or a way using a sucker (Fukuda et al. 1990, Hirose 1986, Ikeda et al. 1992, Ikeda 1994, Luk et al. 1990) or way by wall surface by propelling power (Nishi 1992, Nishi et al. 1992, 1994) etc. have been proposed formerly to Item (1). As a characteristic of the way using a magnet, a control system is simple, and possesses the advantage that standstill action stabilizes. But there is the disadvantage of limited quality of the object structure. Considering equipment such as vacuum equipment, such as sucker, and an inhalant mechanism etc, there is the big advantage because quality of a wall surface is not considered. Moreover, concerning a way by propelling power, burden to a controlling device becomes big with respect to stability of standstill action.

A walking formula (Ikeda, 1994, Luk et al. 1990, Hivose et al. 1992), a crawler formula (Oomichi 1992, Nagatsuka 1986), a wheel formula (Nishi 1992, Nishi et al. 1992) etc have been proposed formerly to Item (2). A walking formula to overcome an obstacle is in general preferable by its

mobility and adaptability to the surfaces. On the other hand, the contrary exists in crawler and wheel formula. For wall surface transfer robots, rapidness of work, certain safety, laborsaving are important for the specified workspace and an optimum form needs to be decided in designing a running mechanism.

Additional primary reasons are in (Oomichi 1992): (1) climbing and descending capabilites are not sufficient to overcome wall surface roughness (adhering to irregular surfaces is generally inadequate); (2) payload and speed are sufficient. High-speed robots have a low load capacity and visa versa; (3) abilities to travel on irregular surfaces (such as steps or sloped terrains) are lacking.

In (Oomichi 1992) existing systems are also examined (see Fig. 5) the crawler type yielding both high-speed and high-load capabilities is determined and proves to be the most practical design given for the present level of technology.

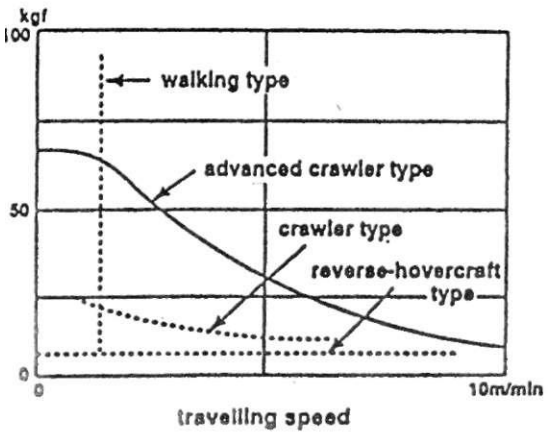

Figure 5. Speed and load characteristics of WCR

In this paper, as an initial step we consider the following conditions in designing a running mechanism of a wall surface mobile robot: (a) quality of a wall surface is not considered; (b) transfer speed is fast; (c) control is easy; (d) robot is light weighted. As a result, in consideration of these point, we adopt the absorption formula with a sucker, and the transfer formula with a crawler. In this paper, the crawler mechanism which possesses multiple suckers on a crawler surface is proposed as optimum fusion form of both promlems (Fukuda et al. 1992, 1992b, 1994).

As a *second step*, for ensuring great carrying capacity and load characteristics of WCR in application to a variety of technological operations we consider a walking type of WCR with pneumatic grippers formed by large suckers type (Gradetsky 1993, Chernousko 1994).

3. WALL SURFACE MOBILE ROBOT HAVING MULTIPLE SUCKERS ON VARIABLE STRUCTURAL CRAWLER

Different approach to vacuum adhering crawler systems nammed "VACS" (Nagatsuka 1986) and their magnetic and pneumatic modifications in (Asami, 1994, Anon 1990, Oomichi et al. 1992, Naito 1992, Aoyama et al. 1992, Fukuda et al. 1990, Chernousko et al. 1994) are discussed. In this paper, we study moving mechanism of a wall surface mobile robot for hazard maintenance under gravity, which can cling to a vertical wall or ceiling using vacuum pads.

The main idea or stable motion of crawler is illustrated in Fig. 6.

Example 1. In ordinary case, the momentum diagram (Fig.6a) at equilibrium

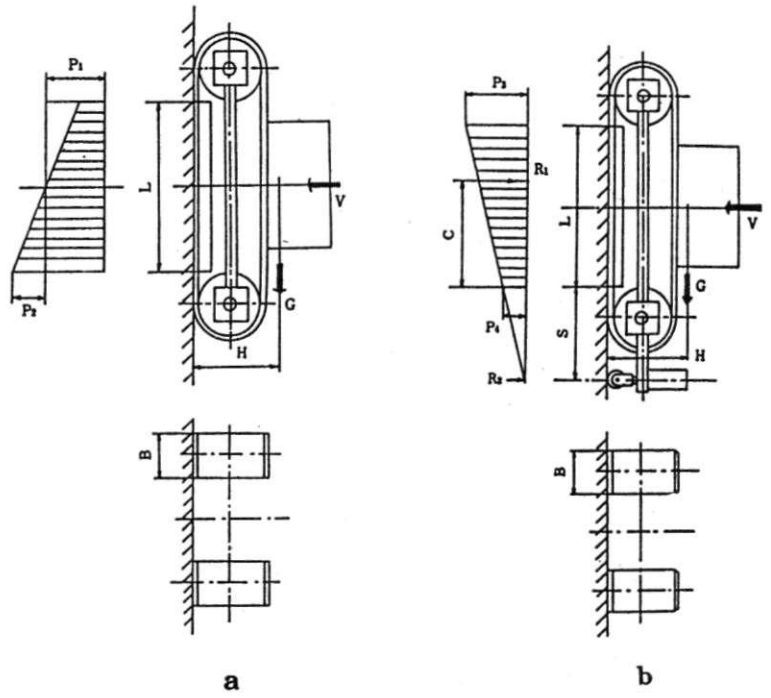

Figure 6. Motion models of crawlers with different load capacity.

(in this case, $p_1 > p_2$) has the following conditions (Nagatsu 1986):

$$p_1 = \frac{V}{2BL};\ p_2 = \frac{GH}{2BL^2/6};\ p_1 > p_2 \text{ and}$$
$$\frac{V}{2BL} > \frac{GH}{2BL^2/6};$$
$$V > \frac{6GH}{L};\ \frac{H}{L} = \frac{1}{2} \quad and\ V > 3G.$$

When stable adhering mechanism is applied, the momentum diagram at equilibrium has the following conditions, and is transformed to form as in Fig. 6b.

$$R_1 = \frac{p_3+p_4}{2} 2BL = p_3(1 + \frac{S}{L+S})BL;$$
$$C = \frac{L}{3}\left(\frac{2+\frac{S}{L+S}}{1+\frac{S}{L+S}}\right);$$
$$R_1 = \frac{V(S+\frac{L}{2})-GH}{S+C};\ R_2 = V - R_1;$$
$$V(S+\frac{L}{2}) > GH;$$
$$V > \frac{\frac{GH}{L}}{\frac{1}{2}+\frac{S}{L}};\ \frac{H}{L} = \frac{1}{2};\ \frac{S}{L} = \frac{1}{2} \quad \text{and}$$
$$V > 0.5G$$

In this case the required force V for backing up of crawler on wall is decreased 6 times.

The first step examines the structure of the crawler (Fig.7) which clinging to vertical wall or to ceilings by means of vacuum pads (Fukuda et al. 1992b). The main body consists of one crawler belt. The guide rail bearings displace through the straight frame of the robot and it is described in Part II. The robot has two pulleys, one of them actuated by a DC motor. The configuration of the crawler cannot be changed in

this case. The vacuum pads are set on the crawler so as to enable rapid mobility on the surface. By this mechanism, the sucking control system becomes quite simple compared with the conventional one (Oomichi et al. 1992). There are 20 suckers installed on the crawler belt.

Based on these ideas, we designed, manufactured and tested the prototype Mark I (Fig. 7), which has fixed structural crawler has $0.514[m]$ length between two wheels, and has a total weight of $4.5[kg]$. In the experiment (Fig.8), Mark I has reached maximum moving speed of 0.05 m/s on the acrylic wall in upward direction. Mark I succeeded in climbing smoothly on the surface of a vertical wall and a ceiling, with both rough and smooth finishes (Fukuda et al. 1992b).

Moreover, we designed another advanced version of the wall surface mobile robot Mark II (Fig.9), which has variable structural crawler (crawler changes its structural configuration). This type of robot can cling firmly to the curved surfaces such as the surface of a tank, can change its direction, can transfer to the other surface, and can get over some small obstacle such a duct on the wall. Mark II which is similar to a caterpillar was manufactured and tested. We provide here some moving experimental results (Fukuda et al. 1992a, 1994).

Mark II is $0.6[m]$ long (maximum total length) and its total weight is $4.6[kg]$ (Fig.9). The crawler belt has multiple suckers (described in Part II). The valve opens automatically when the mechanical switch touches the surface, and closes soon after detaching. The configuration of the belt has to change so as to bend on the body, so the belt has cutting and is decsribed in Part II. There are 25 suckers on the crawler belt.

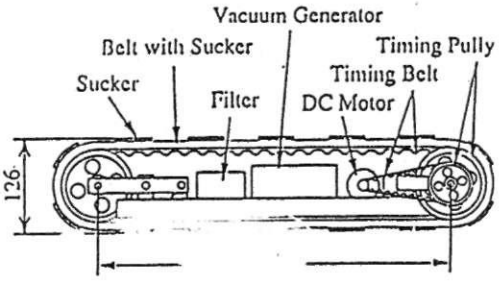

Figure 7. Mark I with fixed structural crawler.

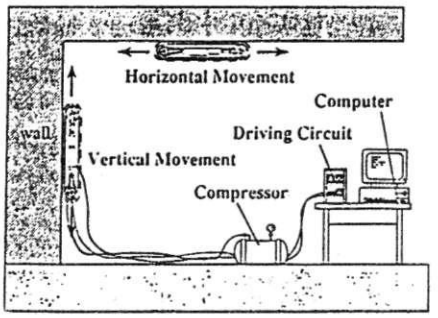

Figure 8. Experiment scheme with Mark I.

The main body consists of one crawler belt, and the main frame is partitioned into several pieces which are connected to each other with springs so that the body can change its configuration without loosing its distribution capability. Here we call this mechanism a multiple jointed frame (for detailed description see (Fukuda et al. 1992a, 1992b, 1994) and Part II). The guide rail bearings go through the partitioned guide frames. The robot has two pulleys and one of them is actuated by a

DC motor. It also has another two DC motors for changing direction and transferring to the other surface. The moving modes of the Mark II are illustrated in Fig. 10. The experiments were performed on acrylic plates for all these four modes (Fig. 10). The experimental results are summarized in Table 1.

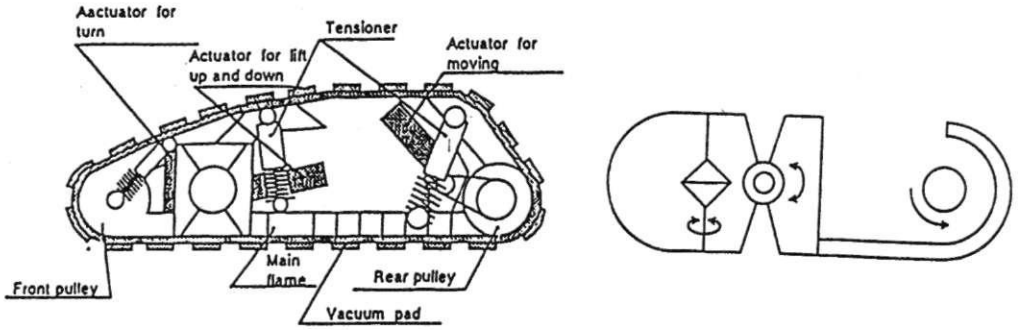

Figure 9. Mark II with variable structural crawler.

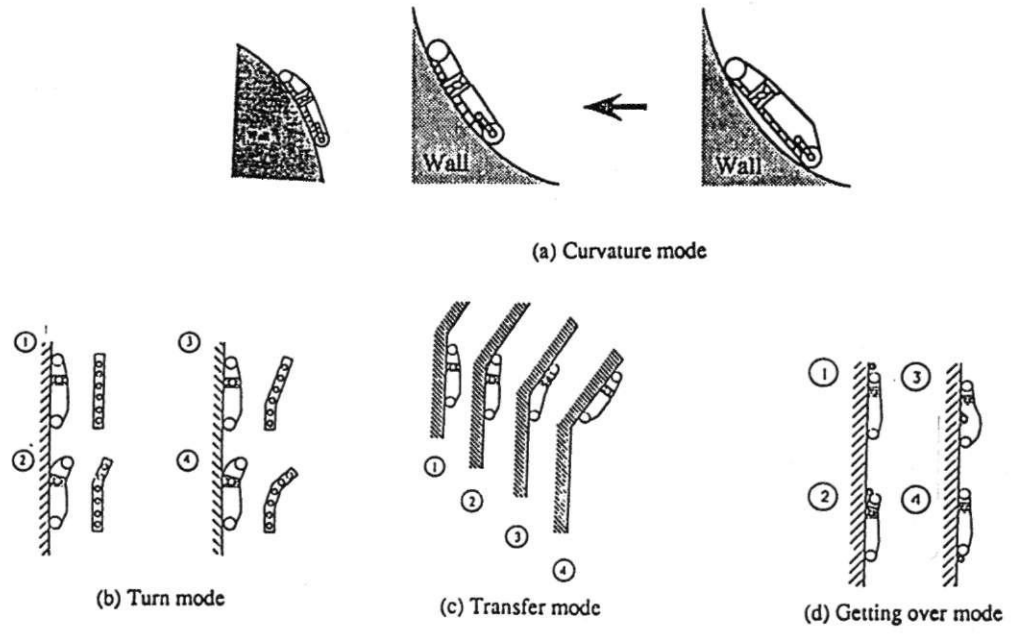

Figure 10. Moving modes of wall surface mobile robot having multiple suckers on variable structural crawler.

Table 1. Runing experiments of Mark II.

Mode	Results	
Curvature	Acrylic	Min. rotary radius:1.2m
	Copper	Min.rotary radius:1.4m
	Aliminum	Min.rotary radius:1.4m
Turning	Rotary radius: from -10° to + 10°	
Transfering from wall to wall	Transfer angle : from 0° to + 20°	
Passing over an obstacle	Max. section of obstacle: 20 mmx 20mm prism	

4. ANALYSIS OF THE WCR MECHANICAL SYSTEM FOR APPLICATION TO A VARIETY OF ENGINEERING PROBLEMS

The structure of the WCR may vary depending on the task executed by it while modular design of the overall system is retained. The primary principles used in modifying the WCR structure can be determined by analysing realizations of the system for applications such as cleaning, painting, decontamination, and inspection. For ensuring of great carrying capacity and load characteristics of WCR for application to a variety of technological operations we consider a walking type of WCR with pneumatic grippers of large suckers type (Gradetsky et al. 1993, Chernousko et al. 1994). In first step we consier equilibrium conditions for WCR on a surface.

4.1 Equilibrium Conditions for WCR on a Surface.

We will examine the very simple scheme of WCR shown in Fig. 11. The robot comprises of a body and legs with feet equipped with pneumatic (vacuum) grippers. Defining the conditions that will *guarantee reliable contact between the feet and the surface when given external forces are applied to the robot* is an important mechanical problem which must be solved if reliable WCR operation is to be ensured. Some approaches to solving this problem will be discussed next. The WCR's load carrying capacity which are the forces that the WCR must exert in order to remain on the suface will be calculated for certain cases.

We choose Cartesion coordinate system $0xyz$ with a fixed plane surface over which the WCR is to move. We superimpose the plane $0xy$ on this surface and direct the z axis toward the WCR (see Fig. 11). We designate the radius vectors of the centers of the feet $i = 1, \cdots, n$ as

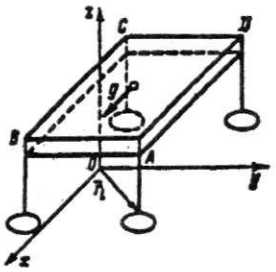

Figure 11. Prototype of WCR

$r_i(x_i, y_i, 0)$. The forces acting on a WCR in equilibrium are as follows.

1) *External active forces* (weight, reaction from the cables, firehoses, and other external objects). We denote the principal vector of these forces $\mathbf{R}$ and their principal moment about the point 0 as M_0.

2) *Normal surface reactions.* We denote the reaction force applied to the i-th foot as $N_i k$, where $\mathbf{k}$ is a unit vector along the z axis, and $N_i \geqq 0, i = 1, \cdots, n$.

3) *Tangential surface reactions (dry friction forces).* We denote the dry friction force acting on the $i-$ th foot as $F_i, i = 1, \cdots, n$. The friction forces lie in the $0xy$ plane and obey Coulomb's law of dry friction:

$$|F_i| \leqq f N_i, (F_i, k) = 0. \tag{4.1}$$

4) *The forces* $\Phi_i k$ by which the feet adhere to the surface due to a vacuum. $i = 1, \cdots, n$. These forces are:

$$\Phi_i = (p - p_i)S > 0, \ i = 1, \cdots, n. \tag{4.2}$$

Here p is the atmospheric pressure, p_i is the pressure under the i-th suction cup, and S_i is its area.

For a WCR being acted upon by applied forces, we write the equilibrium conditions as

$$\begin{aligned} R + \sum[(N_i - \Phi_i)k + F_i] = 0, \\ M_0 + \sum r_i[(N_i - \Phi_i)k + F_i] = 0 \end{aligned} \tag{4.3}$$

and project them onto the coordinate axis. The summation is done everywhere over i from 1 to n. We obtain two groups of equilibrium equations:

$$\begin{aligned} R_z + \sum(N_i - \Phi) = 0, \\ M_x + \sum y_i(N_i - \Phi_i) = 0, \\ M_y - \sum x_i(N_i - \Phi_i) = 0 \end{aligned} \tag{4.4}$$

$$\begin{aligned} R_x + \sum X_i = 0, \\ R_y + \sum Y_i = 0, \\ M_z + \sum(x_i Y_i - y_i X_i) = 0 \end{aligned} \tag{4.5}$$

Here the projections onto the x, y, z axes of the $\mathbf{R}$ and M_0 vectors, respectively, are denoted by R_x, R_y, R_z and M_x, M_y, M_z, and the projections of the F_i forces onto the x, y axes are denoted by X_i, Y_i.

Example 2. *Stable Equilibrium State* of WCR on Wall.

As a particular case of Eqs. (4.3)-(4.5) we discuss here the conditions of stable equilibrium of WCR on a wall for the scheme in Fig.12. In this case the equations for determining stable equilibria are:

$$\left.\begin{aligned} 2N_{fi} + 2N_{f2} + 2N_{r1} + 2N_{r2} - 4F_s = 0 \\ 2f_{f1} + 2f_{f2} + 2f_{r1} + 2f_{r2} - W = 0 \\ -2N_{f1}(l + l_s) + 2(F_s - N_{f2})l - 2N_{r1}l_s - Wh = 0 \end{aligned}\right\} \tag{4.6}$$

with constraints:

$$\left.\begin{aligned} f_{f1} \leqq \mu N_{f1} \\ f_{f2} \leqq \mu N_{f2} \\ f_{r1} \leqq \mu N_{r1} \\ f_{r2} \leqq \mu N_{r2} \end{aligned}\right\} \tag{4.7}$$

In this case the force W is

$$W \leqq 4\mu F_s. \tag{4.8}$$

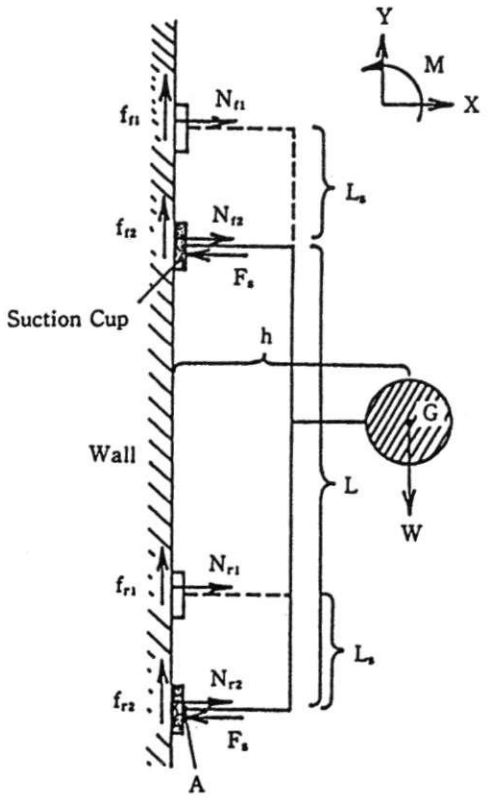

Figure 12. WCR with suction cups.

and we have the condition

$$N_{f2} = N_{r2} = 0 \tag{4.9}$$

substituting Eq. (4.9)in Eq, (4.8) we obtain

$$\left.\begin{aligned} N_{f1} &= (1 - \tfrac{2l_s}{l})F_s - \tfrac{h}{2l}W \\ N_{r1} &= (1 + \tfrac{2l_s}{l})F_s + \tfrac{h}{2l}W \end{aligned}\right\} \tag{4.10}$$

From Eq. (4-10) the force F_s can be determined and for a force W becomes

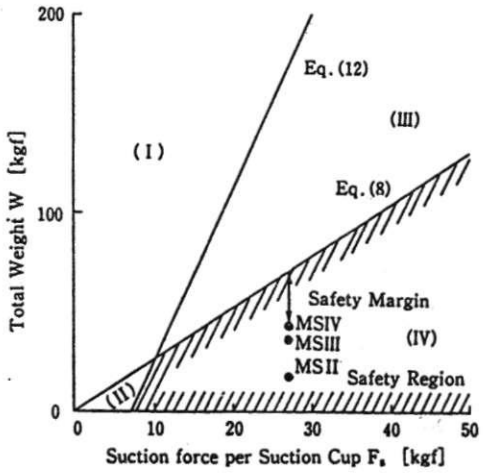

Figure 13. Load capacity and safety region for WCR.

$$W = \frac{2l}{h}\left\{(1 - \frac{2l_s}{l}F_s - F\right\}. \tag{4.11}$$

Fig. 13 illustrates the safety definition of permissible total weight W for WCR in dependence of suction force per suction cup.

Let us indicate the conditions for which a solution exists for the N_i system of equations given by (4.4) that will satisfy the inequalities $N_i \geqq 0$. To do this, we consider a point K on the x, y plane, relative to which the x, y components of the principal vector of the external forces and the Φ_i forces are zero. The radius vector $r^\star$ of the point K is $r^\star = (x^\star, y^\star, 0)$,

$$x^\star = \frac{\sum x_i\Phi_i + M}{\sum \Phi_i - R_x}, y^\star = \frac{\sum y_i\Phi_i - M_x}{\sum \Phi_i - R_x} \tag{4.12}$$

The following is a familiar statement. If the conditions

$$\sum \Phi_i > R_x, \quad K = (x^\star, y^\star) \in D \quad (4.13)$$

are staified, where D is a region in the xy plane and is a convex hull of all the points of contact, then the system given by Eq. (4.4) has a solution for which all $N_i \geqq 0$. The conditions given by Eq. (4.7) are the necessary and sufficient conditions under which a perfectly rigid robot will not come loose from the plane of contact.

In order for a robot to remain in equilibrium, conditions given by Eq. (4.13) should be satisfied and slipping should not occcur. This means that, when rotating about any instantaneous center $C_0(x, y)$ in the plane of contact, the moment of the extenral active forces should not be greater than the moment of the frictional forces. This condition, with respect to Eq. (4.1), is

$$|M_x - xR_y + yR_x| \leqq \sum \rho_i |F_i| \leqq f \sum \rho_i N_i,$$
$$\rho_i = [(x - x_i)^2 + (y - y_i^2)]^{\frac{1}{2}}, \ i = 1, \cdots, n. \quad (4.14)$$

The left-hand side of Eq. (4.14) is the moment of the active forces about an axis passing through the point C_0 parallel to the z axis. The distance from the point C_0 to the i-th point of contact is denoted by ρ_i. The necessary and sufficient conditions for no slipping to occur for a known N_i is

$$sup_{x.y}|Q| \leqq f,$$
$$Q = (M_x - xR_y + yR_x)(\sum \rho_i N_i)^{-1}. \quad (4.15)$$

The maximum here is choosen for all x, y, including a point at infinity, that corresponds to the translational motion. If the conditions given by Eq. (4.13) and Eq. (4.15) are satisfied for the known normal reactions $N_i \geqq 0$, then the WCR will be in equilibrium.

Remark 1. Notice, that Eq. (4.4) forms a set of three equations in n unknowns. Therefore, in general, when $n > 3$ the system is statically indeterminate and the N_i reactions are not uniquely determined. Additional considerations are needed in mechanics for statically indeterminate situations to find the N_i reactions: elastic deformations and geometric imperfections (manufacturing defects) are taken into consideration. When this is done, the result obtained (the distribution of the normal reactions) turns out to be highly dependent upon the rigity of the body and support, and also upon the geometric imperfections.

We now consider some possible methods for further analysis of the equilibrium conditions.

Example 3. *A perfectly Rigid Model.*
Additional data regarding the rigidity of WCR construction and manufacturing defects are not considered so that system remains statically indeterminate. In this case the WCR is said to be statically indeterminate and the N_i reactions can be distributed in a manner that satisfies Eq. (4.4). In this situation, we write the condition for nonslipping, Eq. (4.14), as

$$sup_{x,y,N_i}|Q| \leqq f. \quad (4.16)$$

Here, just as in Eq. (4.14), the x, y can take any value and the N_i's can be

of any values that satisfy Eq. (4.4) and the condition $N_i \geqq 0$. If Eq. (4.13) and Eq. (4.16) are satisfied, the WCR will be in equilibrium for any allowable reaction N_i. For this reason, these conditions are quite naturally called the conditions for *guaranteed equilibrium.*

For verifying these conditions an algorithm has been developed (Chernousko et al. 1994, Abarinov et al. 1989).

A verifying algorithm. We present an algorithm for verifying these conditions.

1) Calculate projections of the principle vector $\mathbf{R}$ and the principle moment M_0 of the external active forces (weight, reactions of the cable and other objects) onto the axis of the $0xyz$ system.

2) Using Eq. (4.2), find the Φ_i forces.

3) Using Eq. (4.12), find the coordinates of the point K.

4) Verify that Eq. (4.13) is satisfied. To execute this taking the size of the foot into consideration we must choose the set D as convex hull of all points of contact. If instead of D a narrow set, namely, a convex polygon $D' \subset D$ with apexes at the centers of the feet r_i is chosen then these conditions will be satisfied within some tolerance. If the points of contact of the legs do not lie on a kingle straight line, then, for reliability it is apparently worthwhile to use the polygon D'; otherwise, D' is a segment and we must now consider the entire set.

5) If either conditions in Eq. (4.13) is violated, the WCR will become detached from the surface. If both conditions are satisfied, we verify the conditions given by Eq. (4.16) in which $\mathbf{Q}$ is found form Eq.(4.15). Verifying Eq. (4.16), presumes that a maximum of the function T has been calculated or estimated; i.e., a number q has been defined such that $sup_{x,y,N_i}|Q| \leqq q$. The condition $q \leqq f$ guarantees that no slipping occurs.

Example 4. *Allowing the Longitudinal elastic Compliance.*
Let us consider a small amount of longitudinal elastic compliance in the WCR legs; i.e., we assume that

$$N_i = -c_i h_i, c_i > 0, i = 1, \cdots, n, \quad (4.17)$$

where h_i is the elongation of the i-th leg and c_i is its rigidity. We denote the displacement along the z axis of a point of the WCR body on the $0z$ axis as h, and the small angles of the body's rotation about the x, y axes as α, β, respectively. the elongation of the i-th WCR leg can then be written as,

$$h_i = h + \zeta_i + (\alpha y_i - \beta x_i) \quad (4.18)$$

Here ζ_i is a small amount of elongation due to structural reasons: the different level of the points at which the legs are attached or the difference in their length within some average value (manufacturing defects). Substituting Eq. (4.18) in Eq. (4.17) yields

$$\begin{aligned} N_i &= -c_i h - c_i y_i \alpha + c_i x_i \beta + N_i^0, N_i^0 \\ &= -c_i \zeta_i. \end{aligned} \quad (4.19)$$

Here, the force N_i^b is equal to the reaction of the i-th leg when the WCR is not displaced relative to its neutral position, i.e., when $h = \alpha = \beta = 0$. Substituting Eq.(4.19) into the equilibrium equation (4.4), yields

$$
\begin{aligned}
&h\sum c_i + \alpha\sum c_i y_i - \beta\sum c_i x_i \\
&= R_z + \sum(N_i^0 - \Phi_i), \\
&h\sum c_i y_i + \alpha\sum c_i y_i^2 - \beta\sum c_i x_i y_i \\
&= M_x + \sum y_i(N_i^0 - \Phi_i), \\
&-h\sum c_i x_i - \alpha\sum c_i x_i y_i + \beta\sum c_i x_i^2 \\
&= M_y \sum x_i(N_i^0 - \Phi_i).
\end{aligned}
\tag{4.20}
$$

Equation (4.20) is system of three linear algebraic equations with three unknowns: h, α, and β. The system of equations (4.20) was solved in (Chernousko et al. 1994).

Remark 2. The solution of the equation (4.20) can be obtained from a transformation of this system. We introduce a point A whose coordinates on the $0xy$ plane are

$$
x_A = \frac{\sum c_i x_i}{\sum c_i}, y_A = \frac{\sum c_i y_i}{\sum c_i}. \tag{4.21}
$$

The point A is the center of mass of a system located at the leg points of contact, and whose mass is proportional to the rigidities c_i of the legs. Assume that

$$
\begin{aligned}
&x_i = x_i' + x_A, y_i = y' + y_A, \\
&h = -\alpha y_A + \beta x_A + h'.
\end{aligned}
\tag{4.22}
$$

From Eqs. (4.21) and (4.22), we obtain

$$
\sum c_i x_i' = \sum c y_i' = 0. \tag{4.23}
$$

Rewriting the system (4.20) and transforming (4.19) using Eq. (4.22) we obtain:

$$
\begin{aligned}
&h'\sum c_i = R_z + \sum(N_i^0 - \Phi_i). \\
&h' y_A \sum c_i + \alpha\sum c_i y_i'^2 - \beta\sum c_i x_i' y_i' \\
&= M_z + \sum y_i(N_i^0 - \Phi_i) \\
&-h' x_A \sum c_i - \alpha\sum c_i x_i' y_i' + \beta\sum c_i x_i'^2 \\
&= M_y - \sum x_i(N_i^0 - \Phi_i) \\
&N_i = -c_i h' - c_i y_i'\alpha + c_i x_i'\beta + N_i^0, \\
&i = 1, \cdots, n.
\end{aligned}
\tag{4.24}
$$

While the determinant

$$
\begin{aligned}
\triangle &= \sum c_i y_i'^2 \sum c_i x_i'^2 - (\sum c_i x_i' y_i')^2 \\
&= \sum \xi_i^2 \sum \eta_i^2 - (\sum \xi_i \eta_i)^2 \geqq 0, \xi_i \\
&= c_i^{\frac{1}{2}} x_i', \eta_i = c_i^{\frac{1}{2}} y_i'
\end{aligned}
\tag{4.25}
$$

is nonnegative because of the Cauchy-Buniakowski inequality, the system (4.24) for α, β has a unique solution (if $\triangle$ is nonzero):

$$
\begin{aligned}
\alpha &= (M_x' \sum c_i x_i'^2 + M_y' \sum c_i x_i' y_i')\triangle^{-1}, \\
\beta &= (M_i' \sum c_i x_i' y_i' + M_y' \sum c_i y_i'^2)\triangle^{-1}.
\end{aligned}
\tag{4.26}
$$

Substituting Eq. (4.26) into Eq. (4.19) yields the unknown normal reaction forces N_i.

The equality $\triangle = 0$ occurs only when the vectors $(\xi_1, \cdots, \xi_n)$ and $(\eta_1, \cdots, \eta_n)$ are colinear. In this case

$$
\frac{y_i}{x_i} = \lambda, \quad i = 1, \cdots, n, \tag{4.27}
$$

which physically means that all of the leg points-of-contact lie on a single straigth line

(λ is a constant): $y - y_A = \lambda(x - x_A)$. Using Eq.(4.27) we find

$$N_i = -c_i h' + c_i x_i' M_y' (\sum c_j x_j'^2)^{-1} + N_i^0, \; i = 1, \cdots, n. \tag{4.28}$$

The equations (4.19) and (4.28) define the amount of longitudinal elastic compliance in the WCR legs.

Remark 3. Note one important circumstance. t is not the absolute values of the rigidities c_i, but their ratios that play the major role in the resultant formulas for calculating the reactions. In fact, in multiplying all c_i by a coefficient $\mu > 0$, the determinant $\triangle$of Eq. (4.25) is multiplied by μ^2, the h', α, β are multiplied by μ^{-1}, and the N_i of Eq. (4.24) and Eq. (4.28) are unchanged. Calculations for the case of identical legs, i.e., when

$$c_i = c > 0, \zeta_i = 0, \quad i = 1, \cdots, n$$

are especially simplified. In this case, the value of c emerges from the resultant formulas and it needs not to be measured.

Remark 4. Notice that in some cases it is adventageous to consider the nonlinearity of the ealstic coupling in Eq. (4.17), i.e., to assume that

$$N_i = -c_i' h_l, \; when \; h_i > 0, N_i = -c"_i h, \; when \; h_i < 0; c_i > 0, c"_i > 0, c_i' \neq c"_i,$$

which, in many cases reflects the true construction features of the robot legs. This complicates the calculations and obliges us to examine different variants.

Modification of verifying algorithm. Thus, when calculating the longitudinal elastic compliance of the robot legs, algorithm for verifying the equilibrium conditions is modified in comparison with the algorithm presented in Example 2. Steps 1)-4) remain unchanged; however, step 5) is replaced by the following procedure.

We are constrained by the rigidities of the legs c_i and by the initial elongations ζ_i. Instead of the ζ_i we can specify the forces $N_i^0 = 0, i = 1, \cdots, n$. If the centers of all the feet are not on a single straight line (the condition $y_i/x_i = \lambda$ is not satisfied) $\triangle \neq 0$ and the reactions N_i are calculated by means of Eqs. (4.24), (4.25) and (4.26); otherwise, when vectors y_i and x_i are colinear ($y_i/x_i = \lambda$) we must verify the condition $M_x'/M_y' = \lambda$ (it is automatically satisfied when $N_i^0 = 0$) and then calculate the N_i according to Eq. (4.28). The condition that no slipping will occur, must then be verified. Here we must calculate a maximum for the Q function, just as we did for the scheme in example 2, but only with respect to the x, y variables, which greatly simplifies our problem.

Other approaches to calculating the equilibrium conditions for a WCR are possible. If, for example, there are structural defects, i.e., torsional rigidities at the points where the legs are attached, we can resort to more complex schemes, one of which will be discussed in the next example.

Example 5. A *Computation Scheme that takes Torsional Rigity into Account.*

We examine still another possible approach to finding the conditions for reliable contact between the feet of a walking WCR and a surface, which allows the necessary calculations to be done in the following two steps.

Step 1. For specific values of the principal vector and principal moment of

external forces applied to the body of the WCR, we find the forces and moments acting upon the grippers at the points where they are connected to the rods, considering all the feet to be surface of moment and that the WCR is in equilibrium.

Step 2. By considering the feet to be perfectly rigid bodies, we find the conditions under which none of them will come loose from the surface, or begin to slip on that surface when acted upon by the forces and moments calculated in Step 1 and the force of the excess atmospheric pressure. Eq. (4.2). The conditions obtained will be taken as the conditions for reliability for reliable contact between the grippers and the surface.

To illustrate this approach, we consider the walking WCR of Fig. 14. The WCR comprises of a body and two pairs of identical legs whose feet are equipped with vacuum grippers. The points at which the legs are attached lie at the vertices of the rectangle ABCD and the cylinders are parallel to the z axis. The contact between each gripper and the plane xy is a circle of radius r. The forces acting upon the WCR are symmetrically distributed over a plane that is perpendicular to the $0xy$ axis and passes through a centerline of the rectangle ABCD. The assumptions allow us to confine ourselves to a "2 dimensional" problem of statics.

The projection of the WCR on the plane of symmetry is shown in Fig.14. We denote the projection of the points of attachment of the first and second pairs of legs to the feet as A_1, A_2 and the points of attachment of these legs to the body of the WCR as B_1, B_2, and choose the point A_1 to be the origin of the rectangular coordinate system A_1xz. We use the following designations: $l = |A_1B_1| = |A_2B_2|$ is the length of the legs; $a = |A_1A_2| = |B_1B_2|$ is the distance between the legs; M is magnitude of the principal moment of external forces applied to the body about the point $B_1; F_x^{(i)}, F_z^{(i)} M^{(i)}, i = 1, 2$ are the projections onto the x, z axes of the principal vector and principal moment of the forces applied to the i-th pair of legs from the cylinder side about the point A_i.

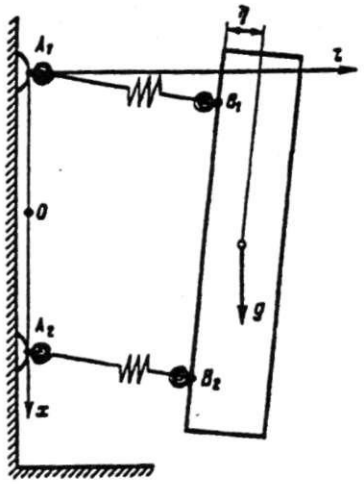

Figure 14. Walking WCR.

The equilibrium conditions for a WCR (considered apart from the feet) being acted upon by external forces and the reactions of the feet are a set of three equations in six unknowns:

$$R_x - F_x^{(1)} - F_x^{(2)} = 0, R_0 - F_z^{(1)} - F_z^{(2)} = 0, M - R_x l - M^{(1)} - M^{(2)} - aF_z^{(2)} = 0.$$

In order to remove the static indetermination, we assume that the legs display

a small amount of elastic compliance on extension and compression, and that their connections to the body and the feet display a small amount of elastic compliance on torsion. The consequence of this is that the WCR body may undergo small displacements relative to the A_1xz coordinate system. We denote the components of the displacement vector for the point B_1 as x, z the angle of the body rotation relative to the A_1xz coordinate system as φ, the coefficients of lengthwise rigidity for a leg in the i-th pair as $c_i, i = 1, 2$, and the coefficients of torsional rigidity at the points A_1, B_1, B_2, A_2 as k_1, k_2, k_3, k_4, respectively.

The potential energy of the small elastic displacements of the WCR is

$$\begin{array}{l}\Pi = \sum_{i=1}^{6} \Pi_i,\ \ \Pi_1 = c_1 z^2, \\ \Pi_2 = c_2(z + a\varphi)^2,\ \ \Pi_3 = k_1(\frac{x}{l})^2, \\ \Pi_4 = k_2(\frac{x}{l} + \varphi)^2,\ \ \Pi_5 = k_3(\frac{x}{l} + \varphi)^2 \\ \Pi_6 = k_4(\frac{x}{l})^2.\end{array} \tag{4.29}$$

Here, Π_1 and Π_2 are the potential energies of the longitudial deformations of the first and second pairs of legs, and $\Pi_3, \Pi_4, \Pi_5, \Pi_6$ are the potential energies of the torsional deformations at the points of attachment A_1, B_1, B_2, A_2, respectively.

The conditions for the WCR body to be in equilibrium when acted upon by external forces and elastic forces with potential energy given by (4.29) are

$$\frac{\partial \Pi}{\partial x} = R_x, \frac{\partial \Pi}{\partial y} = R_y, \frac{\partial \Pi}{\partial \varphi} = M. \tag{4.30}$$

We can uniquely determine the equilibrium position of the WCR body, i.e., the quantities x, y, φ, from the system of linear equations given by Eq. (4.30). The forces and moments acting on the feet at the equilibrium position are found from:

$$\begin{array}{l}F_x^{(i)} = \frac{\partial \Pi_{2i+1}}{\partial x} = \frac{\partial \Pi_{2i+2}}{\partial x} F_z^i = \frac{\partial \Pi_i}{\partial z},\ i = 1, 2; \\ M^{(1)} = \frac{\partial \Pi_4}{\partial \varphi} + xF_z^{(1)} - (l + z)F_x^{(1)}; \\ M^{(2)} = \frac{\partial \Pi_2}{\partial \varphi} + \frac{\partial \Pi_5}{\partial \varphi} + (x - a)F_z^{(2)} \\ \qquad -(l + z)F_x^{(2)}.\end{array} \tag{4.31}$$

Analysis of Eqs. (4.29)-(4.31) shows that as $c_i \to \infty, k_j \to \infty (i = 1, 2; j = 1, 2, 3, 4)$ the elastic displacements tend to zero $(x \to 0, y \to 0, \varphi \to 0)$ and the forces and moments of eq. (4.31) tend to finite limits:

$$\begin{array}{ll}F_x^{(1)} & = [k_1 + k_2(L_1 - L_2)]/(c_2 l^2 \triangle), \\ F_x^{(2)} & = [k_4 + k_3(L_1 - L_2)]/(c_2 l^2 \triangle), \\ F_z^{(1)} & = (\Gamma_1 - 1)\{[a^2\Gamma_2 + \Gamma_3 l^2(\Gamma_2 - \Gamma_3)]R_z \\ & \quad +\Gamma_3 laR_x - \Gamma_2 aM\}\triangle^{-1}, \\ F_z^{(2)} & = R_z - F_z^{(1)}, \\ M^{(1)} & = -k_1 L_1/(c_2 l\triangle), M^{(2)} \\ & = -k_4 L_1/(c_2 l\triangle), \\ \Gamma_1 & = 1 + c_1/c_2, \\ \Gamma_2 & = (k_1 + k_2 + k_3 + k_4)/(c_2 l^2), \\ \Gamma_3 & = (k_2 + k_3)/(c_2 l^2), \\ L_1 & = [a_2(\Gamma_1 - 1) + \Gamma_3 l^2 \Gamma_1]R_x \\ & \quad +\Gamma_3 laR_x - \Gamma_3\Gamma_1 lM, \\ L_2 & = l(\Gamma_1\Gamma_3 lR_x + a\Gamma_2 R_z - \Gamma_1\Gamma_2 M), \\ \triangle & = a^2\Gamma_2(\Gamma_1 - 1) + l^2\Gamma_1\Gamma_3(\Gamma_2 - \Gamma_3).\end{array} \tag{4.32}$$

Direct verification shows that the forces and moments of Eq. (4.32) satisfy the conditions given for the WCR body to be in equilibrium.

We write the equilibrium conditions of Eq. (4.13) and the conditions of nonslipping for a single (the i-th) foot as:

$$\begin{array}{c}F_a^{(1)} \geqq F_z^{(i)}, |M^{(i)}| \leqq r(F_a^{(i)} - F_z^{(i)}), \\ |F_x^{(i)}| \geqq f(F_a^{(i)} - F_z^{(i)}),\end{array} \tag{4.33}$$

The system given by Eq. (4.33) can be conveniently written in the form

$$F_a^{(i)} - F_z^{(i)} \geqq max(|F_x^{(i)}|/f, |M^{(i)}|/r). \tag{4.34}$$

Equation (4.34) in conjunction with Eq. (4.32) are the conditions for reliable contact between the feet and the surface.

In performing the calculation, it is more convenient to calculate the principal moment of the external forces not about the point B_1, as was done above, but about point 0 located at the center of the segment A_1, A_2. The principal moments **M, M*** about the point $B_1, 0$ are related by:

$$M = aR_z/2 + lR_z + M^\star. \tag{4.35}$$

Remark 5. We will give concrete form to the relationships of Eq.(4.34) for typical cases [23].

A. *The rigidities and torsion are small in comprison with the longitudinal rigidity:* $k_1 = k, i = 1,2,3,4; c_j l^2 \gg k, j = 1,2.$

Going to the limit as $k/(c_j l^2) \to 0$ in Eqs. (4.32) and (4.34) we obtain

$$\begin{aligned} M^\star \geqq\ & aR_z/2 - F_a^{(1)} a - lR_x/2 \\ & + a|R_x| max[l/(4r), 1/(2f)], \\ M^\star \leqq\ & -aR_z/2 + F_a^{(2)} a - lR_x/2 \\ & - a|R_x| max[l/(4r), 1/(2f)]. \end{aligned} \tag{4.36}$$

B. *the longitudinal rigidities are small in comparison with the torsional rigidities:* $c_1 = c_2 = c; k_i = k, i = 1,2,3,4; c_j l^2 \ll k.$

When this happens, Eq. (4.34) becomes

$$\begin{aligned} F_a^{(i)} \geqq\ & R_z/2 + max[|R_x|/(2f), \\ & |M^\star/2r], i = 1,2. \end{aligned} \tag{4.37}$$

C. *The torsional rigidities at the points where the legs are attached to the WCR body are small:* $k_i \ll c_j l^2, j = 1,2, i = 2,3, k_1 = k_4.$

The conditions for reliable contact between the feet and the surface are in this case:

$$\begin{aligned} M^\star \geqq\ & aR_z/2 - F_a^{(1)} a - lR_x/2 \\ & + a|R_x| max[l/(2r), 1/(2f)], \\ M^\star \leqq\ & -aR_z/2 + F_a^{(2)} a \\ & - lR_x/2 - a|R_x| max[l/(2r), 1/(2f)]. \end{aligned} \tag{4.38}$$

D. *The torsional rigidities where the feet are attached to the legs are small:* $c_1 = c_2 = c;\ k_2 = k_3 = k,\ k_i \ll cl^2,\ i = 1,4.$

In this case the equilibrium conditions for the feet are

$$\begin{aligned} M^\star \geqq\ & aR_z/2 - aF_a^{(1)} + a|R_x|/f, \\ M^\star \leqq\ & -aR_z/2 + aF_a^{(2)} - a|R_x|/f. \end{aligned} \tag{4.39}$$

E. *The torsional rigidities where the feet are attached to the legs, as well as the longitudinal rigidity of one pair of legs are small:* $k_1 = k_4, k_2 = k_3, k_1 \ll c_2 l^2,$ $k_1 \ll k_2, c_1 \ll c_2, k_1 \sim c_1 l^2.$

Going to the limit as $k_1/k_2 \to 0, k_1/(c_2 l^2) \to 0, c_1/c_2 \to 0,$ in Eqs. (4.32) and (4.34) we obtain

$$\begin{aligned} F_a^{(1)} \geqq\ & \tfrac{c_1 a}{c_1 a^2 + 2k_1} \left(\tfrac{a}{2} R_z - M^\star\right) \\ & + max\left[\tfrac{|R_x|}{2f}, \tfrac{k_1}{r(c_1 a^2 + 2k_1)} \left|\tfrac{a}{2} R_z - M^\star\right|\right], \\ F_a^{(2)} \leqq\ & \tfrac{(c_1 a^2 + 4k_1) R_z 2 c_1 a M^\star}{2(c_1 a^2 + 2k_1)} \\ & + max\left[\tfrac{|R_x|}{2f}, \tfrac{k_1}{r(c_1 a^2 + 2k_1)} \left|\tfrac{a}{2} R_z - M^\star\right|\right]. \end{aligned} \tag{4.40}$$

4.2. Determing the load carrying capability of WCR.

We present the result of calculations for a WCR (Chernousko et al. 1994) that has the structure described in Example 4 and shown in Fig. 14. The geometric parameters of the WCR are: $l = 0.044m$ (the length of a leg); $a = |AD| = 0.344m; b = |AB| = 0.151m; r = 0.034m$ is the distance from the WCR's center of mass to the plane at which the legs are attached to the WCR body. The atmosheric pressure p is taken as $1.01.10^5 Pa$ /760 mm Hg static), and coefficient of friction, f as 0.5, which corresponds to the friction of rubber on a concrete surface. The forces acting on the grippers, Eq. (4.2), are

$$\Phi_i = \Phi = \gamma p \pi r^2 = 366.8\gamma(N), \quad \gamma = (p - pi)/p < 1. \tag{4.41}$$

Let us calculate the maximum mass (including payload) that the WCR can support on a vertical wall. We assume that $\gamma = 0.9$. For simplicity, we also assume that no external force acts upon the WCR except weight, and that the WCR is oriented so that the force of gravity g is directed along the side AD parallel to the x axis (Fig.14). In this case, the simplifying assumptions made regarding the symmetrical distribution of external loads are valid.

Example 6. *Perfectly rigid model.*

We perform the calculations initially using the perfectly rigid model described in Example 2. We place the origin of the coordinate system at the center of the rectangle formed by the points of contact at the centers of the feet and with the plane $0xy$. The coordinates x_i, y_i of the centers of the feet and the components of the principal moment of active forces are

$$\begin{gathered} x_1 = x_2 = -a/2,\ x_3 = x_4 = a/2, \\ y_1 = y_4 = -b/2, y_2 = y_3 = b/2, \\ R_x = mg, R_y = 0,\ R_z = 0, \\ M_x = 0,\ M_y = mg(l+\eta),\ M_z = 0. \end{gathered} \tag{4.42}$$

Equations (4.4) used find to the normal reaction are

$$\begin{gathered} N_1 + N_2 + N_3 + N_4 = 4\Phi, \\ -N_1 + N_2 + N_3 - N_4 = 0, \\ -N_1 - N_2 + N_3 + N_4 = 2mg(l+\eta)/a. \end{gathered} \tag{4.43}$$

It follows from Eq. (4.43) that

$$\begin{gathered} N_1 + N_2 = 2\Phi - mg(l+\eta)/a, \\ N_3 + N_4 = 2\Phi + mg(l+\eta)/a, \end{gathered}$$

$$N_1 + N_4 = N_2 + N_3. \tag{4.44}$$

The coordinates given by Eq. (4.12) for the point K are

$$x^\star = mg(l+\eta)/(4\Phi), y^\star = 0. \tag{4.45}$$

Obviously, the first of the conditions given by Eq. (4.13) is satisfied, and the second is given by the inequality $x^\star < a/2$. Considering Eq. (4.41) and (4.45) we obtain

$$m \leqq m_0 = \frac{2a\Phi}{g(l+\eta)} \doteqdot 274.0\gamma \doteqdot 246.6kg. \tag{4.46}$$

The function $Q(x, y)$ in Eqs. (4.15) and (4.42) is equal to

$$Q = mgy(\sum p_i N_i)^{-1}. \tag{4.47}$$

We will calculate an exact upper bound, Eq. (4.16), for the function given

by Eq. (4.46). From Eqs. (4.43), (4.15), and the last equation of (4.44) we have

$$\begin{aligned}&\sum p_i N_i \geqq \sum |y - y_i| N_i \\ &= |y + b/2|(N_1 + N_4) + |y - b/2|(N_2 + N_3) \\ &= (N_1 + N_4)x(|y + b/2| + |y - b/2| \\ &\geqq 2|y|(N_1 + N_4) = |y| \sum N_i.\end{aligned}$$

From this and from Eq. (4.46) it follows that

$$|Q| \leqq mg(\sum N_i)^{-1}. \tag{4.48}$$

On the other hand, going to the limit as $y \to \infty$, in Eq. (4.47) we find an equality is achived in Eq. (4.48) when this is done. Therefore, taken the first equation of (4.41) into account we have

$$sup|Q| = mg(\sum N_i)^{-1} = mg/(4\Phi). \tag{4.49}$$

We write the nonslipping conditions from (4.41) as $mg/(4\Phi) \ll f$ and, with the help of Eq. (4.41), transform it to

$$m \leqq m_\star = 4\Phi f g^{-1} = 74.9\gamma = 67.4\text{kg}. \tag{4.50}$$

The conditions for guaranteed equilibrium in the case being examined are given by Eqs. (4.46) and (4.50). Because $m_0 > m_\star$, the load carrying capability of the WCR is defined by the quantity $m^\star$.

Example 7. *Longitudinal elasticity of WCR legs.*

We now use the scheme described in Example 3, where only the longitudinal elasticity of the WCR legs is considered. We will say that the coefficient of longitudinal rigidity for all legs is c. Then Eqs. (4.21), (4.24) and (4.26) yield:

$$\begin{gathered}x_A = y_A = 0,\ h' = -\Phi/c, \\ M'_x = 0,\ M'_y = -mg(l + \eta), \\ \triangle = c^2 a^2 b^2, \\ \alpha = 0,\ \beta = mg(l + \eta)/ca^2), \\ N_1 = N_2 = \Phi - mg(l + \eta)/(2a), \\ N_3 = N_4 = \Phi + mg(l + \eta)/(2a).\end{gathered} \tag{4.51}$$

It is apparent from Eq. (4.51) that $N_3 > 0, N_4 > 0$ for any m and $N_1 > 0, N_2 > 0$ only when $m < m_0$; (see Eq. (4.46)). Because the N_i satisfy the last equation of (4.44), the maximum of the function $Q(x, y)$ coincides with Eq. (4.49).

Thus, calculations done according to the scheme discussed in Example 2 yield the same result that was found by the scheme in Section 3.1:

$$m \leqq m_\star = 67.4\text{kg}. \tag{4.52}$$

Example 8. *The computing scheme with torsional rigidity.*

We now calculate the maximumn allowable mass using the scheme given in Example 4 for the various relationships between longitudinal and torsional rigidities. In making the transition to the "planar" model, we assume that $F_a^{(1)} = F_a^{(2)} = 2\Phi$, where Φ has been calculated according to Eq. (4.41) and $M^\star = -mg(l + \eta)$. We perform the calculations according to Eqs. (4.36)-(4.40) for cases A-E in Example 4.

A. The inequalities

$$\begin{aligned}&mgl + 2\eta + amax[l/(2r), 1/f] \leqq 4\gamma p\pi r^2 a, \\ &mgamax[l/(2r), 1/f] - l - 2\eta \leqq 4\gamma p\pi r^2 a\end{aligned}$$

follow from the condition given by (4.36) and, consequently,

$$\begin{aligned}m \leqq m_\star^A &= \frac{4\gamma p\pi r^2 a}{g\left\{\left[l+2\eta+amax\left(\frac{l}{(2r)}, \frac{1}{f}\right)\right]\right\}} \\ &= 61.9\gamma = 55.7 \text{ kg}.\end{aligned} \tag{4.53}$$

B. From Eq. (4.47) we have

$$mgmax\left[\frac{1}{f}, \frac{l+\eta}{r}\right] \leqq 4\gamma p\pi r^2$$

and, consequently,

$$\begin{aligned} m &\leqq m_\star^B = \tfrac{4\gamma p\pi r^2}{gmax[1/f,(l+\eta)/r]} \\ &= 54.2\gamma = 48.7 \text{ kg}. \end{aligned} \tag{4.54}$$

C. For the case being examined, Eq. (4.48) has the forms

$$\begin{aligned} mgl + 2\eta + amax[l/1, 1/f] &\leqq 4\gamma p\pi r^2 a, \\ mgamax[l/r, 1/f] - l - 2\eta &\leqq 4\gamma p\pi r^2 a, \end{aligned}$$

and the maximum allowable mass is found from the relationship

$$\begin{aligned} m &\leqq m_\star^C = \tfrac{4\gamma\pi r^2 a}{g[l+2\eta+amax(l/r,1/f)]} \\ &= 61.9\gamma = 55.7 \text{ kg}. \end{aligned} \tag{4.55}$$

D. The conditions given by Eq. (4.49) lead to

$$\begin{aligned} mg[2(l+\eta) + a/f] &\leqq 4\gamma p\pi r^2 a, \\ mg[a/f - 2(l+\eta)] &\leqq 4\gamma p\pi r^2 a, \end{aligned}$$

from which it follows that

$$\begin{aligned} m &\leqq m_\star^D = \tfrac{4\gamma f p\pi r^2 a}{g[a+2f(l+\eta)]} = 58.8\gamma \\ &= 52.9 \text{ kg}. \end{aligned} \tag{4.56}$$

E. This situation corresponds to that in which the rigidity of the legs in extension is much less than in compression (see the comment in Example 2). From Eq. (4.40) we have

$$\begin{gathered} mg2(l+\eta)g_1(v) + max[1/f, 2(l+\eta)g_2(v)/r] \leqq a\gamma p\pi r^2, \\ g_1(v) = [a(1+2v)]^{-1}, 9_2(v) = v/(1+2v), \\ v = k_1/(c_1 a^2) \end{gathered}$$

and consequently,

$$m \leqq m_\star^E = \frac{4\gamma p\pi r^2}{g(2(1+\eta)g_1(v) + max[1/f, 2(l+\eta)g_2(v)/r])}. \tag{4.57}$$

Remark 6. Analysis of the $m_\star^E(v)$ function at an extremum shows that:

1) if $f(l+\eta) \leqq r$, then $m_\star(v)$ increases monotonically and $sup_{v>0} m_\star(v) = lim_{v\to\infty} m_\star(v) = 4\gamma p\pi r^2 f/g$;

2) if $f(l+\eta) > r$ and $a < 2r, m_\star^E(v)$ increases monotonically and $sup_{v>0} m_\star^E(v) = lim_{v\to\infty} m_\star^E(v) = 4\gamma p\pi r^2/[g(l+\eta)]$;

3) if $f(l+\eta) > r$ and $a \geqq 2r, m_\star^E(v)$ has a single maximum when $v > 0$:

$$\begin{aligned} &max_{v>0} m_\star^E(v) \\ &= m_\star^E(v_\star) = 4\gamma p\pi r^2 af/g[2f(1+\eta) - 2r + a \\ &v_\star = 1/2r[f(l+\eta) - r]^{-1}. \end{aligned} \tag{4.58}$$

The parameters of the model being examined correspond to situation 3), and the maximum load carrying ability of the WCR with respect to v is calculated ac-

cording to Eq. (4.58)

$$m_\star^E(\upsilon_\star) = 69.6\gamma = 62.6 \text{ kg}, \ \upsilon_\star = 1.3. \tag{4.59}$$

Here $m_\star^E$ increases monotically from 58.8γ to the value given by Eq.(4.9) when υ is varied from 0 to υ_{star}, and then decreases monotonically, tending to 54.2γ as $\upsilon \to \infty$.

From here it follows that the load carrying capability of a WCR can be increased significantly by optimal choice of the structural rigidity parameters. Equations (4.52)-(4.59) show that the design maximum payload that a WCR can carry without coming loose and slipping depends upon the structural parameters.

A calculation scheme for a given WCR must be chosen with respect to the relationship between its structural and operating parameters. In keeping uith these conditions the WCR route, which includes the type of step, and the track (where the feet are placed) must be chosen. The calculation schemes discussed above can be performed on a computer and used to verify the reliability of contact between the WCR and the surface over the entire path that the WCR traverses. When this is done, the verifiable inequalities must be provided with sufficient reserve to compensate for inaccuracies in the initial data.

5. ANALYSIS OF STABLE GRASPING STRATEGY FOR WCR

When WCR starts its operations in any goal position the creation of vacuum to keep the WCR body in equilibrium will depend on its posture. It is very important that before starting operations WCR body must be held in most stable posture. So for a number of research work for generation of stable grasping strategies (Li et al. 1988, 1989, Nguyen 1989, Salisbury 1981) have been carried out. But all are devoted to multi-fingered robot hands in manipulating type of robots. However, in this paper stable grasping strategies for WCR based on two quality measures (Petrov et al. 1978): structured twist space quality measure (T_q) and structured wrench space quality measures (R_q), have been found out. Other quality measures may also be included (Gradetsky et al. 1991), but for simplicity and to illustrate the principle here the stable grasping strategy based on T_q and R_q have been considered.

5.1. Analysis of Stable Grasping Strategy for WCR.

Contact kinematics and transformation relations in this case are following. Let us consider the following coordinate frames: C_w- the inertial frame, i.e., the reference frame attached to the wall; C_R- the body coordinate frame attached with the erasping gripper of the WCR body; C_{li}- the leg coordinate frame attached with the last link of the leg; C_{Li}- the local coordinate frame attached with the i-th point of contact with the leg of the wall; C_{wi}- the instantaneous fixed coordinate frame relative to the wall attached at the i-th point of contact.

Note that the Z axis of C_{Li} and C_{wi} coincide, Φ is defined to be the contact angle relative to the two X axes. This is function of contact geometry.

Now it is well known that the operator

$$T(w) = \begin{bmatrix} 0 & -w_3 & w_2 \\ w_3 & 0 & -w_1 \\ -w_2 & w_1 & 0 \end{bmatrix}$$

where

$$w = \begin{bmatrix} w_1 \\ w_2 \\ w_3 \end{bmatrix}$$

when operated on the radius vector

$$f_s = \begin{bmatrix} f_1 \\ f_2 \\ f_3 \end{bmatrix}$$

gives the following results

$$T(w)f_s = [wXf]_s = -[fXw]_s T(f_s)w;$$

Using this result and transformation principle we have deduced the force/troque and velocity transformation relations between WCR body to leg tips and leg tips to the leg joints. The results have been summarized below in Table 2 and shown in the Fig.15.

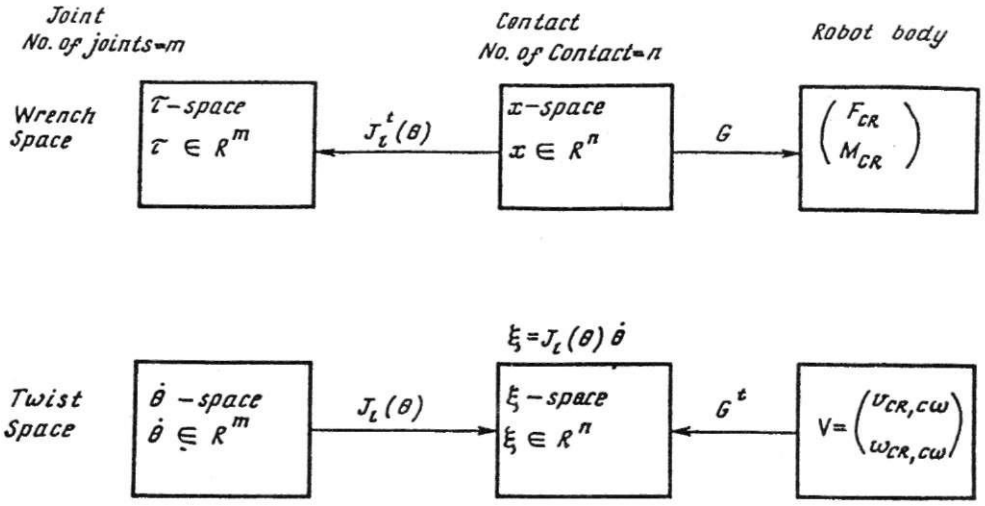

Figure 15. Transformation relations in wrench and twist spaces.

Table 2. Transformation relations between WCR body to leg tips and leg tips to the leg joint.

	Force/Torque Relations	Velocity Relations
Robot body to leg tips	$\begin{pmatrix} F_{CR} \\ M_{CR} \end{pmatrix} = GX$	$\xi = G^t \begin{pmatrix} V_{CR,Cw} \\ W_{CR,Cw} \end{pmatrix}$
Leg tip to joints	$\tau = J_l^t(\theta)X$	$\xi = J_l(\theta)\dot{\theta}$

where G - grasp matrix,
X - the contact wrench,
ξ - the contact velocity vector,
$J_l(\theta)$ - leg Jacobian of the robot.

With this background we shall now try to evaluate the two quality measures T_q and R_q.

5.2 Grasp Planning.

There are two main steps for grasp planning : 1) selecting a good grasp on the wall; and 2) using the cooperative action of the legs to take the WCR body in a proper grasping position.

In this part we shall study how to generate the good grasp based on two quality measures: *twist space quality measure* and *wrench space quality measure.* Then the performance is being measured by constructing *the performance measurement function* $PM = f(T_q, R_q)$,

$$PM = T_q^{\gamma} R_q^{1-\gamma} \tag{5.1}$$

where the value of γ will depend on the type of work the system will perform.

As an example, for stable grasping function, more weightage should be given to wrench space quality measure R_q rather than manipulability quality which is characterized by twist space quality measure T_q. Then we have choosen the values of γ as 0.2.

Evaluating of twist space and wrench space quality measures. Our next step is to evaluate T_q and R_q. Let us model the gripping task by two task ellipsoids E_T and E_R, one in twist space and anotler in the wrench space. Also let us assume stiffness control is used for the WCR legs. Hence leg σ_i is related to δ_i by $\sigma_i = K_i \delta_i$, where K_i is the desired stiffness in the direction D_i- the task direction expressed in body coordinate.

In the generalized form we can represent

$$E_T = \alpha E_1 X + c \tag{5.2}$$

and

$$E_R = \beta E_2 X + d \tag{5.3}$$

where α and β are the scaling parameters responsible for the size of the ellipsoids, E_1 and E_2 are the structured matrix given by

$$E_1 = [D_1, \cdots, D_6] \begin{bmatrix} \delta_1 & \cdots & 0 \\ \vdots & \vdots & \vdots \\ 0 & \cdots & \delta_6 \end{bmatrix} \begin{bmatrix} D_1^t \\ \vdots \\ D_6^t \end{bmatrix} = D \delta D^t \tag{5.4}$$

and

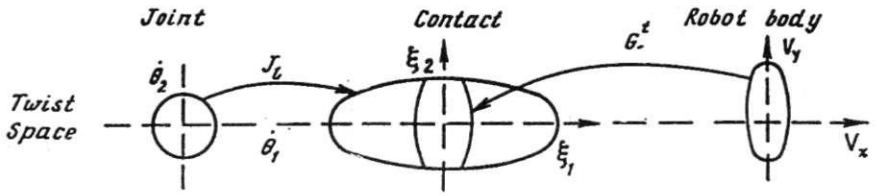

Figure 16. Structured twist space quality measure T_q.

$$E_2 = [D_1, \cdots, D_6] \begin{bmatrix} \sigma_1 & \cdots & 0 \\ \vdots & \vdots & \vdots \\ 0 & \cdots & \sigma_6 \end{bmatrix} \begin{bmatrix} D_1^t \\ \vdots \\ D_6^t \end{bmatrix} = D\sigma D^t \tag{5.5}$$

$X, c, d \in R^6, |X| \leqq 1$; for simplicity we shall assume $c = d = 0$.

A. Structured Twist Space Quality Measure T_g.

Let us assume a unit ball in $R^m(O_1^m \subset R^m)$, the space of leg joint velocities, and define the structured twist space quality T_q by

$$T_q = Sup_{\alpha \in R}\alpha, \quad \text{such that } j_1(O_1^m) \supset G^t(E_T) \tag{5.6}$$

The physical meaning of T_q is as follows. The unit ball O_1^m in the leg joint velocity space is mapped into the space of contact velocity by J_1. On the other hand, gripping task ellpsoid is mapped back into contact velocity space by G^t. Function T_q is then the largest α such that $G^t(E_T)$ is contained in $J_l(O_1^m)$ (see Fig.16). In other words the WCR body velocity of size α can be accomodate by leg joint velocity of unit magnitude.

Theoretically T_q is the ratio of structured output (the task ellipsoid) over the input (i.e., the leg joint velocity).

From Fig. 16, it is evident that T_q is at its maximum if the inner ellipsoid has the same size and orientation as the outer ellipsoid. Now using the expression $J_l(O_1^m) = \alpha E_1 X \in R^n, \langle \alpha E_1 X, (J_l J_l^t)^{-1} \alpha E_1 X \rangle \leqq 1$ and $G^t(E_T) = \{\alpha G^t E_1 X \in R^n : X \in R^6 | X| \leqq 1\}$.

From Eq. (5.6),we have $G^t(E_T) \subset J(O_1^m)$ if and only if $\langle \alpha G^t E_1 X, (J_l J_l^t)^{-1} \alpha G^t E_1 X \rangle \leqq 1$ for all $|X| \leqq 1$, or, $\alpha^2 \sup \langle G^t E_1 X, (J_l J_l^t)^{-1} G^t E_1 X \rangle \leqq 1$, or $\alpha^2 \sup < X, / G^t E_1)^t (J_l J_l^t)^{-1} G^t E_1 X \leq 1$ which is equivalent to s

$$\alpha \leqq \sigma_{max}^{-1/2} \{E_1^t G (J_l J_l^t)^{-1} G^t E_1\} \tag{5.7}$$

or, $\alpha \leqq \sigma_{\max}^{-1/2} M, where M = \{E_1^t G (J_l J_l^t)^{-1} G^t E_1\}$ and $\sigma_{max} M$ is maximum singular value of the matrix M. Hence from (5.6),

$$T_q = \sigma_{max}^{-1/2} M \tag{5.8}$$

B. Structured Wrench Space Quality Measure R_q.

To evaluate wrench space quality measure R_q let $O_1^n \subset R^n$ be unit ball in the leg wrench space and $\sigma_{\max}(J_l)$ be the maximum singular value of J_l. We define the structured wrench space qaulity

$$R_q sup_{\beta \in R}(\beta, \text{ such that } G(O_1^n) \supset E_R).\sigma_{max}^{-1}(J_l) \tag{5.9}$$

The physical meaning of R_q has been elaborated in the Fig.17. As before it can be evaluated as

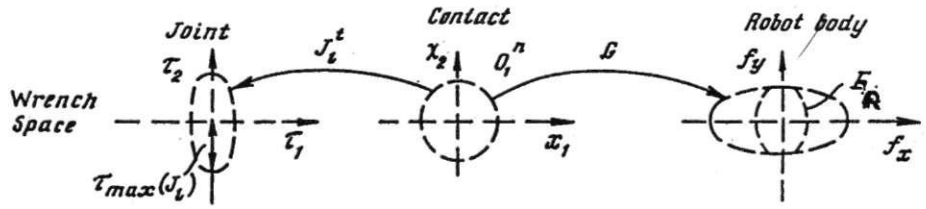

Figure 17. Structured wrench space quality measure R_q.

$$R_q = \sigma_{max}^{-1/2}\{E_2^t(GG^t)^{-1}E_2\sigma_{max}^{-1}(J_1)\} = \sigma_{max}^{-1/2}N \tag{5.10}$$

where

$$N = E_2^t(GG^t)^{-1}E_2\sigma_{max}^{-1}(J_1)$$

C. Determination of Stable Posture.

After calculating the matrices M and N, T_q and R_q can be evaluated by the singular decomposition data of the matrices. Then the posture matrix (PM) incorporating T_q and R_q is to be evaluated. Then we will have to draw the following curves: posture (Θ_{ij}) vs. $T_q; \Theta_{ij}$ vs. R_q and 0_{ij} vs PM, and we shall select that posture (Θ_{ij}) corresponding to what T_q, R_q and PM will be maximum.

5.3. Results of Simulation.

For simplicity let us consider a two dimensional model. Let: 1) the contact be modelled as point contact with friction; 2) the leg spacing be of two unit; 3) G is fixed; and 4) the WCR body is constrained to move vertically, This leaves the system with a single degree of freedom. Let Θ_{ij} be the generalized coordinate of the system and we study how Θ_{ij} affects the structured grasp quality measure.

Construction of Grasp Matrix G. Steps which are to be followed for constructing the grasp matrix are: 1) specify a body coordinate and obtain the coordinates of each contacting point; 2) determine the unit normal and two orthogonal tangent vectors to the contact point; 3) pick up a torque origin in body coordinates and the particular choice of the torque origin.

Computation for Leg Jacobian:

$$J_L = LegJacobian = \begin{pmatrix} J_{L1} & 0 \\ 0 & J_{L2} \end{pmatrix}$$

where

$$J_{L1} = \begin{pmatrix} Cos\alpha & -Sin\alpha \\ Sin\alpha & Cos\alpha \end{pmatrix} \begin{pmatrix} -Sin\theta_{11} & -Sin(\theta_{11}+\theta_{12}) & -Sin(\theta_{11}+\theta_{12}) \\ Cos\theta_{11} & Cos(\theta_{11}+\theta_{12}) & Cos(\theta_{11}+\theta_{12}) \end{pmatrix}$$

$$J_{L2} = \begin{pmatrix} -Cos\alpha & Sin\alpha \\ -Sin\alpha & -Cos\alpha \end{pmatrix} \begin{pmatrix} -Sin\theta_{21} & -Sin(\theta_{21}-\theta_{22}) & Sin(\theta_{21}-\theta_{22}) \\ Cos\theta_{21} & Cos(\theta_{21}-\theta_{22}) & Cos(\theta_{21}+\theta_{22}) \end{pmatrix}$$

where $\alpha = 0$ the orientation angle of the WCR body; other constraints are $\Theta_{12} = \pi - 2\Theta_{11}, \Theta_{21} = \pi - 0_{11}$ and $0_{11} - 0_{22} = \pi - (\Theta_{11} + \Theta_{12})$.

Other Computations. Value of

$$K = \begin{pmatrix} 10 & 0 & 0 \\ 0 & 190 & 0 \\ 0 & 0 & 100 \end{pmatrix}, D = I,$$

unit matrix.

$$\delta = diag\{0.8\ 0.7\ 0.02\}; \sigma = diaq\{8\ 133\ 2\}.$$

For two contact points the grap matrix

$$G = \begin{pmatrix} -1 & 0 & 1 & 0 \\ 0 & -1 & 0 & 1 \\ 0 & -1 & 0 & -1 \end{pmatrix}$$

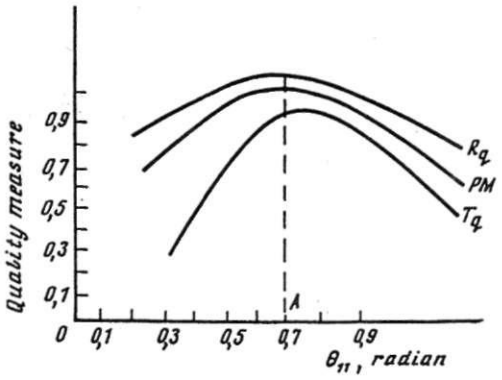

Figure 18. Quality measures T_q, R_q and performance measure PM as function of Θ_{11}.

Knowing D, δ and σ, structured matrices E_1 and E_2 can be computed from Eqs. (5.4) and (5.5), hence we can calculate T_q and R_q from Eqs. (5.8) and (5.10) respectively by singular value decomposition data of M and N. Figure 18 shows plots of quality measure and the performance measure as a function of Θ_{11}. It is evident from Fig. 18 that the optimal posture of WCR corresponds to the position A where $\Theta_{11} = 0.7$ radian (40 degrees approximately).

6. CONCLUSIONS

Significant attention in many countries has recently been focused on the design of robots for service use, which has independent robotic capable of movement under complex conditions in the presence of obstacles. In this process the organization of robot motion along vertical or inclined surfaces with reliable adhesion to these surfaces represents one of the fundamental theoretical problems, since such surfaces represent an important part of many different structures. The capacity to travel along such surfaces requires the robot to maintain significant adhesion forces that must be rapidly and reliability controlled by the control system. One of important areas in such research is the improvement of grippers, particularly, vacuum grippers. For moving on surface of complex configuration, which includes horizontal and vertical section, it is more important to develop combined mobile systems that contain WCR and horizontally-mobile robot with linkages. The wide variety of possible mobile systems is due both the extensive range of travelling surfaces and the variety of industrial problems requiring specific equipment. Combining such a equipment, as well as the required sensors, with a mobile transport system also represents a serious problem. In this light, the development of mobile robots capable of climbing vertical or

other complex surfaces represents a fundamental theoretical problem with a wide variety of applications.

Concerning running experiments, we represented the robot moving quickly and smoothly on a wall surface and on a ceiling. With variable structural crawler mechanism, the wall surface mobile robot can cling firmly to the curvature, change its direction, transfer to the other surface, and get over some obstacle.

The development of the scientific field concerned with the construction of integrated WCR and horizontally-mobile robot with an advanced sensor system will require additional capabilities including autonomous decision-making on advancement in vague environments under extreme situations. In these cases, complex mobile robotic systems must incorporate elements of an advanced intelligent system. Hence supervisory control used today will, as robot system advance, be gradually replaced by more entilligent control that will be capable of solving such problems in changing of extreme conditions.

REFERENCES

Abarinov A.V., Akselrod B.N., Bolotnik N.N. et al. (1989). "A robot system moving over vertical surfaces", *Soviet Journal of Computer and System Sciences*, **27** (2): 130-142.

Abe T. (1992). "Wall climbing robot for inspection of concrete structure", *Journal of Robotics Society of Japan*, 10(5): 590-593.

Anon (1990). *Robot Olympics (Glasgow'90), First International Robot Olympics*, University of Strathclyde, Glasgow, UK.

Aoyama H., Iwasaki T., Sasaki A., and Shimokohbe A. (1992). "Micro climber with piezo thrust and magnectic lock", *Proceedings of International Symposium on Theory of Machines and Mechanism (IFToMM-jc)*, Nagoya, Japan, **1**: 282-287.

Asami S. (1994). "Robots in Japan: Present and future (The new generation of service robot)", *IEEE Robotics and Automation Magazine*, 1(2): 22-26.

Chernousko F.L. (1994) Bolotnic N.N. and Gradetsky V.G., *Manipulation Robots: Dynamics, Control, and Optimization*, CRC Press Inc., NY.

Fukuda T., Arai F., Matsuura H. and Nishibori K. (1992). "Wall surface mobile robot having multiple suckers on variable structural crawler", *Proceedings of International Symposium on Theory of Machines and Mechanism (IFToMM-jc)*, Nogoya, Japan, **2**: 707-712.

Fukuda T., Hosoki H. and Shimasaka H. (1990) "Autonomous plant maintainance robot (Mechanism of Mark IV and its actuator characteristics)", *Proceedings of IEEE International Workshop on Intelligent Robots and Systems'90 (IROS'90)*, Nagoya, Japan, **1**: 471-478.

Fukuda T., Nishibori K., Matsuura H., Arai F., Saski S. and Kanasige M. (1994). "A study of wall surface mobile robot (2nd Report, Mechanism of model with variable structural

crawler and running experimental results)", *Transaction of Japan Society Mechanical Engineers,* **60** (569C): 21-217.

Fukuda, T., Nishibori K., Matsuura H., Arai F., Saki S. and Kanasige M. (1992b). "A study of wall surface mobile robot (1st Report, Development of moving mechanism for crawle type of wall surface mobile robots with vacuum pads)", *Transaction of Japan Society Mechanical Engineers,* **58** (550C): 1972-1979.

Gradetsky V.G., Rachkov M. Yu. and Ulyanov S.V. et al. (1993). "Mobile systems with wall climbing robots", *Journal of Computer and Systems Sciences. International,* **31**(1): 126-142.

Gradetsky V.G., Rachkov M.Yu., Ulyanov S.V. and Nandi G. (1991). "Robots for cleaning and decontamination of building construction", *Proceedings of 8th ISARC,* Stuttgardt, Germany, **1**: 257-266.

Hirose S. (1986). "The development of sucker mechanism for wall climbing robot", *Robot (JIRA),* (54): 53-57.

Hirose S., Nagakubo A. and Toyama R. (1992b). "Legged wall-climbing robot", *Journal of Robotics Society of Japan,* **10**(5): 575-580.

Hirose S., Tsutsumitake H., Toyama R. and Kobayashi K. (1992a). "Development of disk rover, wallclimbing robot using permanent magnetic disk", *Journal of Robotics Society of Japan,* **10**: 992-997.

Ikeda K. (1994). "Wall climbing robot with SSC", *Journal of Japan Hydraulics and Pneumatics Society,* **25** (5): 638-641.

Ikeda K., Nozaki T. and Shimada S. (1992). "Development of self-contained wall-climbing robot", *Journal of Mechanical Engineering Laboratory of Japan Government,* **46** (2): 128-137.

Li Z. and Sastry S. (1988). "Task oriented optimal grasping by multifingered robot hands", *IEEE Journal of Robotics and Automation,* **4**(1): 38-47.

Li Z., Hsu P. and Sastry S. (1989). "Grasping and coordinate manipulation by a multifingered robot hand", *International Journal of Robotics Research,* **8** (4): 342-348.

Luk B.L., Colli A.A. and Billingsley J. (1990). "ROBUG II: An intelligent wall climbing robot", *Proceedings of IEEE International Journal of Robotics and Automation,* pp.2342-2347, 1991; and "Design and performance of the portsouth climbing robot", *Proceedings of 7th ISARC,* Bristol, UK: 235-239.

Nagatsuka K. (1986). "Vacuum adhering crawler system"VACS", *Robot (JIRA),* (53): 127-135.

Naito S. (1992). "Wall surface robot with magnetic crawlers", *Journal of Robotics Society of Japan,* **10**: 606-608.

Nguyen D. (1989). "Constructing stable grasp", *International Journal of Robotics Research,* **8** (1): 26-34.

Nishi A. and Miyagi H. (1992). "A wall climbing robot using propulsive force of propeller", *Transaction of Japan Society Mechanical Engineers,* **57**(543C), pp. 3585-3591; **58**(547C): 837-843.

Nishi A. and Miyagi H. (1994). "A computer-control system using wireless controller (an application to wall-climbing robot)", *Proceedings of 7th Intelligent Mobile Robot Symposium'94,* Atsugi, Japan,(940-252): 60-63.

Nishi A.(1992) "Development of wall-climbing robot", *Robot(JIRA)* (84). pp. 11-116, 1992; and "Wheel or crawler type wall-climbing robot", *Journal of Robotics Society of Japan,* **10**(5): 570-574.

Oomichi T., Ike T., Nakajima M., Hayashi K., and Takemoto Y. (1992) "The wall inspection robot with adaptive mechanism for wall surface", *Proceedings of International Symposium on Theory of Machines and Mechanism (IFToMM-jc),* Nagoya, Japan, **1**: 336-341.

Petrov B.N., Ulanov G.M. and Ulyanov S.V. (1978). *Theory of Modelling in Control Processes,* Nauka Press, Moscow, (in Russian).

Salisbury J.K. (1981). "Articulated hands: Force control and kinematic issues", *Proceedings of Joint Automatic Control Conference,* Virginia, USA: 367-369.

Yamafuji K., Yamazaki Y., Watanabe T., Ogino K., Hamura M. and Seaki K. (1992). "Development of intelligent mobile robot for service use", *Proceedings of Japan Society Mechanical Engineers Annual Conference on Robotics and Mechatronics (ROBOMEC'92),* Kawasaki, Japan, B: 269-270.